

# A $^{13}\text{C}$ NMR Study of the Condensation Chemistry of Acetone and Acetaldehyde Adsorbed at the Brønsted Acid Sites in H-ZSM-5

A. I. Biaglow,<sup>\*,1</sup> J. Šepa,<sup>\*</sup> R. J. Gorte,<sup>\*</sup> and David White<sup>†</sup>

<sup>\*</sup>Department of Chemical Engineering and <sup>†</sup>Department of Chemistry, University of Pennsylvania, Philadelphia, Pennsylvania 19104-6323

Received June 30, 1994; revised September 22, 1994

Several bimolecular, acid-catalyzed condensation reactions of acetone and acetaldehyde have been examined in H-ZSM-5, along with the adsorption complexes formed by the products, using  $^{13}\text{C}$  NMR. For acetone, the hydrogen-bonded adsorption complex is stable at room temperature and coverages below one molecule per Brønsted acid site. Reaction to mesityl oxide occurs only at higher coverages or temperatures, which are necessary to induce site exchange. The adsorption complex exhibits reaction chemistry analogous to that observed in solution phase, forming adsorption complexes of chloroacetone upon exposure to  $\text{Cl}_2$  and of imines upon exposure to  $\text{NH}_3$  or dimethylamine. The reactions of acetaldehyde to crotonaldehyde and imines are similar, although they occur at a faster rate due to the higher mobility of this molecule. The adsorption complexes formed by acetone, acetaldehyde, and their condensation products can all be described as rigid, hydrogen-bonded complexes at low coverages. Complexes formed from imines and enamines exhibit isotropic chemical shifts nearly identical to those observed in magic acids, indicating that proton transfer is nearly complete for these molecules. The extent of proton transfer for the remaining molecules varies with the proton affinity of the molecule, ranging from close to complete proton transfer for mesityl oxide and crotonaldehyde to almost complete absence of proton transfer for the chloroacetones. The differences and similarities between these reactions in the zeolite and in solution phase are discussed, along with the implications for understanding the primary processes responsible for these reactions in zeolites. © 1995

Academic Press, Inc.

## INTRODUCTION

There are many examples of acid-catalyzed reactions which occur in zeolites, many of which have important industrial applications. There is, however, also the potential of employing such "solid acids" in organic synthesis via acid-catalyzed condensation reactions (1–3) such as have been extensively studied in liquid solutions (4, 5). While the mechanisms that describe the reaction pathways for the elementary processes are reasonably well understood in solution, we can only speculate on the fundamental microscopic processes in zeolites by analogy

with solutions. The two situations are quite different. Whereas the primary process in zeolites is the formation of an adsorption complex at the Brønsted site with partial (hydrogen-bonded) or complete transfer of a proton to an adsorbed molecule, the initial step in acid solutions can be described by an equilibrium between protonated and unprotonated species defined by a  $\text{p}K_a$  (6, 7). While the adsorption complex in the zeolite, localized at the Brønsted site, is also thermally equilibrated in its environment, proton displacements here should only be thought of as small fluctuations mediated by phonons in the lattice rather than proton exchange reactions satisfying microscopic reversibility. Furthermore, while the activation energies for the elementary processes that define the reaction pathways at the Brønsted sites are determined by barriers along reaction coordinates defined by the framework, the effects of solvation dominate in the case of acid–base chemistry in liquid solutions.

With high-activity zeolite catalysts at loadings and temperatures corresponding to actual reaction conditions, the elementary processes typically proceed far too rapidly to be spectroscopically observable using NMR techniques. These processes, which involve delocalization and thus an equilibrium between molecules at Brønsted and physisorbed sites, can be slowed by controlling the site exchange surface dynamics involving the Brønsted sites as demonstrated in our studies (6, 7) as well as the pioneering studies of condensation reactions in H-ZSM-5 by Bosacek *et al.* (8, 9). The results of those studies demonstrate that control of both temperature and surface coverage is critical for understanding the reactivity of species interacting with the Brønsted sites. In particular, coverage effects, which are often not considered in detail, can greatly decrease the temperatures necessary for bimolecular reaction, change the initial products which are observed in reaction, and otherwise affect the mobility of the adsorbed molecules (10). Since coverage is so important, any scale of zeolite reactivity, even a qualitative scale, must take into account surface coverage and exchange dynamics, which differ for different adsorbates and adsorbents.

<sup>1</sup> Current address: Department of Chemistry, West Point Military Academy, West Point, New York.

The present studies are an extension of the work of Bosacek *et al.* and include the condensation reactions of both acetone and acetaldehyde under somewhat different conditions and with zeolites having higher Si/Al ratios. In our study, the condensation reactions have been investigated at lower temperatures and under *in situ* conditions where the surface coverages with respect to the number of Brønsted sites, as distinct from the number of equivalents of Al in the zeolite, are controlled. These are conditions under which the surface species prior to reaction have been well defined (6, 7, 11). Since the acid-base reactions of interest are taking place at the Brønsted sites, of critical importance has been the work in our laboratories in establishing the existence of stoichiometric 1:1 adsorption complexes associated with these sites in H-ZSM-5 (11–14). This provides a basis for characterizing the zeolite with respect not only to the number of Brønsted sites, which can be considerably less than the number of equivalents of aluminum in the zeolite, but, equally important, also to the loadings beyond which the adsorption complex is ill defined due to site exchange with physisorbed species (6).

From our earlier  $^{13}\text{C}$  NMR studies of the adsorbed acetone molecule, the picture of the complex that emerges, not only in H-ZSM-5, but also in other high-catalytic-activity zeolites, such as H-Y, H-ZSM-12, H-ZSM-22, and mordenite (6, 7), is one of stabilization and localization at low temperatures of a surface species by the formation of a hydrogen bond. Furthermore, the Brønsted sites in these zeolites are characterized by a unique rather than any broad distribution of acidities; i.e., the sites in these zeolites are nearly identical. This is confirmed by NMR studies in the "rigid lattice" regime for H-ZSM-5 that show:

- (i) the anisotropy of the carbonyl  $^{13}\text{C}$  shift tensor as a well-defined nonaxially symmetric powder pattern;
- (ii) the anisotropy in the  $^{13}\text{C}$  spectrum persists even at room temperature, but becomes motionally narrowed due to molecular reorientations when the surface coverage is greater than one molecule per Brønsted site;
- (iii) the elements of the shift tensor are independent of the zeolite loadings, providing that the surface coverage is less than one molecule per Brønsted site; and
- (iv) the trace of the chemical shift tensor (isotropic shift) is 17 ppm downfield from that of  $^{13}\text{C}$  carbonyl in solid acetone and independent of temperature at these low surface coverages.

The formation of a hydrogen-bonded complex can be inferred from the changes in the components of the shift tensor relative to pure solid acetone as well as the magnitude of the isotropic shift (15). This is also supported by preliminary theoretical SCF calculations at the Hartree-Fock level, with geometry optimization under the

constraint of  $C_s$  symmetry, for the acetone adsorption complex where the zeolite is simulated by the model cluster  $\text{H}_3\text{SiOHAlH}_2\text{O Si H}_3$  (16). The calculated O-H hydrogen bond length is 1.83 Å. The calculated isotropic chemical shift is 14 ppm downfield from that of molecular acetone using the TEXAS-90 program of Pulay (17). This is in good agreement with the measured isotropic shift of acetone on H-ZSM-5 (6–10). Since the "cluster" representing the Brønsted site is nonspecific with respect to the zeolite, it is interesting to note that the range of chemical shifts for the previously noted high-catalytic-activity zeolites is from 12 to 18 ppm (7), in good agreement with theory. Calculations are now under way in which the constraints of  $C_s$  symmetry are removed and correlations at the MP-2 level are included.

In this article, we examine the conditions that initiate the condensation reactions in H-ZSM-5. We show that the initial bimolecular processes involving hydrogen-bonded complexes of acetone and acetaldehyde at Brønsted sites, following the onset of site dynamics by increasing surface coverage or thermal activation, lead to the formation of new surface complexes, whether it be the formation of carbocations or hydrogen-bonded precursors to carbocations driving the reaction. Results for aldol condensations of a single component are presented, followed by two component condensations involving substituted ammonias. From these studies, as well as those of Bosacek *et al.* (8, 9), it is shown that a consistent picture concerning the mechanism of such elementary processes in the solid acids can be obtained.

## EXPERIMENTAL

Two H-ZSM-5 samples were used in this study, H-ZSM-5(A) and H-ZSM-5(B). Since the results are identical for each of these samples, results are shown mainly for sample H-ZSM-5(A). This sample was synthesized hydrothermally with an Si/Al ratio of 35, according to the method of Rollman and Valyocsik (18), using tetra-*n*-propylammonium bromide as a template, and is the sample used in Refs. (6) and (7). The concentration of Brønsted acid sites on each sample was measured using temperature-programmed desorption (TPD) and thermogravimetric analysis (TGA) (11) and was 370  $\mu\text{mol/g}$  for H-ZSM-5(A). The ZSM-5B sample was obtained from Standard Catalyst Committee and had a site density of 520  $\mu\text{mol/g}$ . The TPD-TGA technique for measuring the concentration of Brønsted acid sites depends on the observation that isopropylammonium ions, formed at the Brønsted acid sites, decompose to propene and ammonia in a well-defined feature centered between 575 and 650 K, whereas physisorbed isopropylamine (in excess of one per Brønsted site) completely desorbs at lower temperatures (11, 14). The TPD-TGA experiment can also be

used as an analytic tool for identifying surface species using mass spectral cracking fractions, and we have used this technique to confirm the identity of crotonaldehyde and mesityl oxide formed from acetaldehyde and acetone, respectively.

For NMR measurements, the H-ZSM-5 samples, approximately 200 mg in size, were degassed and weighed at 700 K in a Cahn microbalance at  $10^{-6}$  Torr. The samples were then transferred to specially designed glass sample tubes and attached to a vacuum manifold, where they were again degassed at 700 K to  $10^{-6}$  Torr. The degassed samples were exposed to controlled amounts of C2, 99%  $^{13}\text{C}$ -enriched acetone (Cambridge Isotope Labs, Inc.) using a calibrated volume to permit the small volumes of adsorbate to be known to within 2%. To avoid bed effects in adsorption, the zeolite was spread along the length of an evacuated,  $\frac{1}{2}$ -in. tube during exposure to the adsorbates and then poured into a smaller tube, without exposure to air. The smaller tube was sealed and inserted into a homebuilt double-resonance static NMR probe for spin-counting measurements, which in all cases were in agreement with the measured dosing volumes. After portions of the samples were transferred in an inert atmosphere to O-ring sealed rotors, magic angle spinning (MAS) spectra were obtained using a Doty probe (DSI-574). Comparison of the *in situ* broad line spectra at low surface coverages (or higher resolution spectra at high surface coverages) obtained in the Doty probe and the static probe in the absence of MAS indicated that there were no measurable changes on transferring of the samples from the sealed NMR tubes to the Doty rotors. Additional confirmation that our experimental procedures result in equilibration of the adsorbates comes from a comparison of our results for acetone in H-ZSM-5 with the observations of Bosacek *et al.* (8, 9), whose sample preparations are very different from those described here, but whose spectra are identical. They achieved a uniform coverage by exposing their zeolite to low coverages of adsorbate ( $\sim 0.2$  molecule/Brønsted site) at elevated temperature (400 K) to promote migration. By contrast, the need to slow the spinning speed in order to observe spinning sidebands in the spectra of Haw and co-workers (10) suggests that local adsorbate coverages in their work may have been in excess of one/Brønsted site. If indeed their surface coverages were uniformly less than one molecule per Brønsted site, then, under the cited conditions of the NMR experiment, there would be no need to decrease the spinning speed to observe sidebands, such as shown in Fig. 1 of Ref. (7).

The  $^{13}\text{C}$  NMR spectra were obtained at a field of 3.5 T (37.48 MHz  $^{13}\text{C}$  resonance frequency) using a homebuilt spectrometer that has been described previously. The lineshapes were determined from the observation of proton-decoupled Hahn echoes and cross-polarization (CP)

spectra. The Hahn echo sequence consisted of a series of  $90^\circ-\tau-180^\circ-\tau$  pulses in quadrature, with a delay time,  $\tau$ , of 30  $\mu\text{s}$ , and a repetition time of 10 s, which was sufficiently long to account for spin-lattice relaxation. The contact time in the CP experiments was 2 ms and the repetition time in these measurements was 1 s. Unless otherwise noted, the NMR spectra were acquired at room temperature, with a dwell time of 5  $\mu\text{s}$ , with 4096 points in the acquisition, and 25 Hz of Lorentzian line broadening added prior to Fourier transforming the data. MAS experiments were conducted at various frequencies up to 4.5 kHz to establish the positions of the spinning sidebands in the spectra.

## RESULTS

The condensation reactions of acetone and acetaldehyde in this paper which will be discussed in this paper can each be described as a nucleophilic attack on the carbonyl carbons in molecules which form complexes with the acid site of the zeolite. As demonstrated by the chemical shifts of the 1:1 complexes, these carbonyl groups are significantly deshielded by hydrogen bonding to the zeolite hydroxyls, and, as a result, the electrophilic properties are enhanced significantly. The nature of this deshielding will be addressed under Discussion. Our description of the results will focus first on the factors which activate the bimolecular chemistry of acetone in H-ZSM-5 and then on the specific reactions which occur (acid-catalyzed aldol condensations). It is generally accepted that the aldol condensation reaction involves the formation of enols, and these are further examined using chlorination reactions. The formation of imines by exposure of chemisorbed acetone and acetaldehyde to ammonia and dimethylamine is addressed in detail.

### Reactions of Acetone

As we have shown previously, the localized adsorption complex does not undergo reaction at room temperature and for surface coverages below one molecule per Brønsted site. (6, 7). This is illustrated in the CP spectrum of acetone at a coverage of 0.88 molecule per Brønsted site (Fig. 1a), which clearly indicates the spinning sidebands (labeled with asterisks) to second order for a MAS frequency of 3.1 kHz. This spectrum shows a single feature at 222 ppm from TMS shifted 17 ppm from pure liquid acetone (205 ppm). The direction of the shift is consistent with what one observes for acetone in pure liquid acids (15), and its magnitude is in the range observed for other molecular sieves examined previously (6, 7). The presence and number of spinning sidebands are consistent with our earlier studies of the chemical shift anisotropy (6, 7) (see Ref. (7) for the components of the chemical shift tensor), which establish that this species is localized

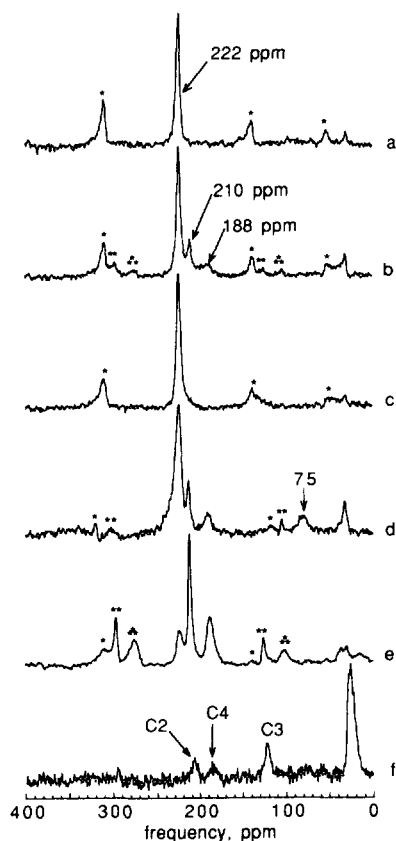
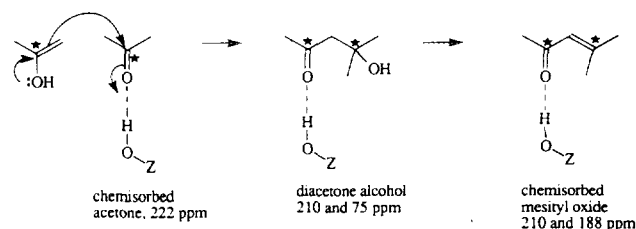


FIG. 1. MAS spectra of acetone adsorbed on H-ZSM-5(A) at 3.2 kHz. Spectrum (a) CP, 0.88 molecule per site; (b) CP, 0.88 molecule per site, after heating to 100°C for 3 h; (c) Hahn echo of sample in (b); (d) CP, 1.50 molecules per site; (e) CP, 1.50 molecules per site, after heating to 100°C for 90 min; and (f) CP, 0.5 molecule of pure, unenriched mesityl oxide per site. Spectra (a) through (e), 16,384 scans. Spectrum (f), 65,536 scans.

on the time scale of the NMR measurement. The small feature at 35 ppm is due to the natural abundance signal of the methyl group in unreacted acetone. (Since cross polarization tends to enhance the peaks due to bimolecular products over that of unreacted acetone, as we will demonstrate shortly, essentially no secondary reactions have occurred in the same in Fig. 1a.)

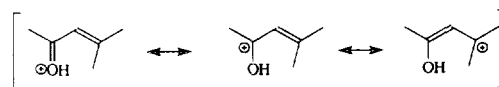
Figure 1b shows the CPMAS spectrum, measured at 295 K, of acetone at a coverage of 0.88 molecule per acid site after the sample had been heated to 100°C for 3 h. The spectrum shows the formation of two new features at 210 and 188 ppm, which have been assigned to the C-2 and C-4 carbons of mesityl oxide (10, 19), a bimolecular reaction product. This appearance of bimolecular products occurs at a temperature and surface coverage at which TPD-TGA studies under UHV conditions have demonstrated that desorption will occur. Therefore, mobility, caused by thermal activation in this case, appears to be a critical factor in the formation of mesityl oxide.



SCHEME 1. Formation of mesityl oxide from acetone.

Another significant aspect of this spectrum is the presence of spinning sidebands for the features assigned to mesityl oxide, which suggest that at room temperature this species is largely static on the time scale of the NMR measurement. The sideband structure associated with the unreacted acetone is identical to that observed in Fig. 1a, consistent with our earlier observation that the lineshape is nearly identical at all coverages less than one per site (6). These features are also observed by Bosacek *et al.* (9). Differences in the results reported by Haw and co-workers (see Fig. 5 of Ref. (10)) appear to be due to higher local coverages.

The bimolecular reaction of acetone to form mesityl oxide is outlined in Scheme 1. Here we have pictured the observed condensation chemistry as a nucleophilic attack on the carbonyl carbon of an "activated," or chemisorbed, acetone by the  $\pi$ -electrons of the enol. Our experiments cannot determine which is the mobile species, nor is it necessary in the elucidation of the elementary process. The double bond in the enol acts as a nucleophile and adds to the carbonyl carbon of acetone, forming diacetone alcohol, with chemical shifts of the labeled carbons at 210 and 75 ppm. (The chemical shift of the carbonyl carbon in diacetone alcohol is similar to that of mesityl oxide, and the spectral features probably overlap.) The diacetone alcohol is not observed in Fig. 1b because it dehydrates rapidly at 100°C to form mesityl oxide. It is observed at lower temperatures, as will be discussed shortly. The exact nature of the chemical shifts of the labeled carbons in mesityl oxide has been rationalized by Olah (20) in terms of the resonance structures shown in Scheme 2. As in the case of Olah's work, the downfield shifts of the carbonyl carbon and the  $\beta$ -carbon adsorbed in H-ZSM-5 at Brønsted sites have been assigned to a hydrogen-bonded precursor to a hydroxyallylic cation of mesityl oxide.



SCHEME 2. Hydroxyallylic carbocations.

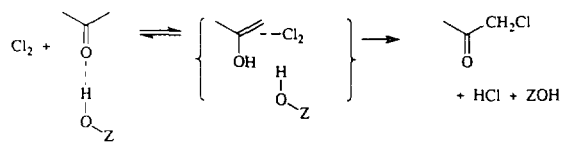
In order to assess the extent of reaction in the spectrum of Fig. 1b, a MAS Hahn echo spectrum in which the spin count was identical (within +5%) to the initial unreacted acetone is shown Fig. 1c. Since the features associated with mesityl oxide are not observed, it is clear that the CP enhancement is large enough to permit the observation of initial products formed at the onset of reaction.

Figure 1d is the 295 K CPMAS spectrum, at 3.2 kHz, of a sample prepared and maintained at room temperature where the surface coverage is 1.5 molecules per Brønsted acid site. (A nearly identical spectrum was obtained at a coverage of 1.08 molecules per Brønsted site.) This again shows the formation of mesityl oxide, but now diacetone alcohol, which is the first product formed from acetone, shown in Scheme 1, can also be observed, as shown by the peak at 75 ppm. It is important to note that the feature at 222 ppm, corresponding to unreacted acetone, is broadened and does not show appreciable spinning sidebands, which indicates "slow motion" mobility (21, 22) at the higher surface coverage. This is in agreement with previously published results which demonstrate the collapse of the shift anisotropy for coverages greater than one molecule per Brønsted site (6). In fact, it appears that it is this mobility at the higher surface coverage that leads to reaction at a lower temperature. Bimolecular products are formed when adsorbate mobility is increased by either temperature or surface coverage.

It is interesting to note that the isotropic chemical shift of the unreacted acetone in Fig. 1d is the same as that in Fig. 1a, even though the shift anisotropy has been dramatically altered. While the adsorbed molecule is now reorienting on the time scale of the NMR measurement, it must still be spending most of the time, on average, in the environment of the Brønsted site (6). While the details of the reorientation dynamics at this surface coverage are not fully understood, one can still speak of stable adsorption complexes at the Brønsted sites. Although the dynamical time scale for the complexes at higher coverages is much shorter than that for the 1:1 complex, they are localized sufficiently long for the acid-catalyzed reaction to occur.

Figure 1e is the 295 K CPMAS spectrum at 3.2 kHz of the same sample examined in Fig. 1d following heating to 100°C for 1.5 h. Longer exposure at 100°C simply produces more mesityl oxide condensate with the disappearance of the diacetone alcohol and unreacted acetone. However, as the reaction nears completion, the number of Brønsted sites accessible for the unreacted acetone increases and this is evidenced by the reappearance of the spinning sidebands comparable in relative intensity to those in Fig. 1a.

Finally, to verify the assignment of the features at 210 and 188 ppm to the C-2 and C-4 carbons of mesityl oxide, the spectrum of isotopically unenriched mesityl oxide on



SCHEME 3. Chlorination of enols.

H-ZSM-5 at a coverage of 0.5 molecule per Brønsted site is shown in Fig. 1f. The 208 and 186 ppm features are similar to those seen in the condensation products formed from the C-1 isotopically enriched acetone. The additional features in the spectrum correspond to the C-3 (123 ppm) and C-1,C-5 (overlapping at 26 ppm) carbons of the unlabeled mesityl oxide.

#### Chlorination of Acetone

The reaction with  $\text{Cl}_2$  is commonly used to look for enol formation since the reaction, outlined in Scheme 3, is generally accepted as occurring via the enol form (23). Figure 2a shows the spectrum obtained after adsorption of 0.50 molecule of acetone per Brønsted acid site on the zeolite, followed by exposure to 40 Torr of  $\text{Cl}_2$  for 15 min at room temperature. The spectrum consists mainly of unreacted acetone (222) ppm, but also shows the formation of a new species giving rise to the chemical shift at 206 ppm. This we assign to chloroacetone (Scheme 3), an assignment which is supported by the spectrum in Fig.

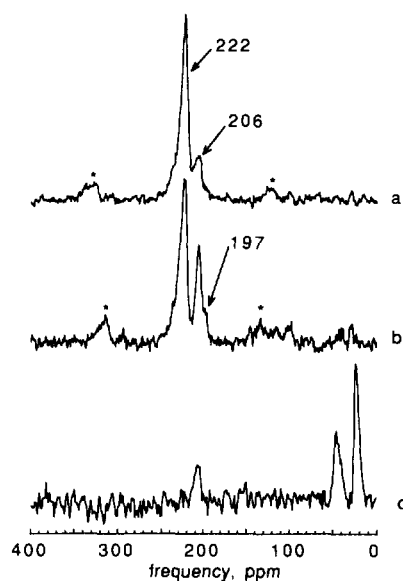
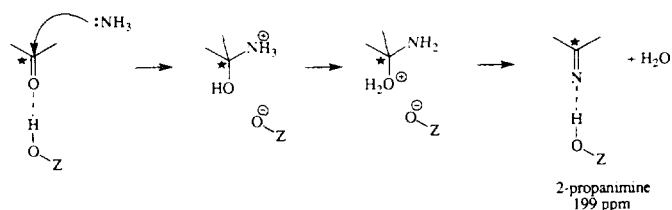


FIG. 2. CPMAS spectra of 0.5 molecule of acetone per site on H-ZSM-5(A) exposed to (a)  $\text{Cl}_2$  for 15 min, MAS frequency 4.5 kHz, 8192 scans, and (b)  $\text{Cl}_2$  for 75 min, MAS frequency 3.5 kHz, 8192 scans. Spectrum (c) was obtained following exposure to pure chloroacetone, 77,600 scans.



SCHEME 4. Formation of 2-propanimine from acetone and ammonia.

2c. The feature at 206 ppm is shifted 5 ppm downfield from pure liquid chloroacetone.

As expected, the spectrum following longer exposure (40 Torr  $\text{Cl}_2$  for 75 min) shows an increase in the concentration of chloroacetone, and we begin to see a shoulder at 197 ppm which we assigned to dichloroacetone, downfield-shifted 2 ppm from the pure liquid. The presence of a feature at 197 ppm was confirmed using cross polarization, which preferentially enhances its intensity in the spectrum. Finally, the assignment of the feature at 206 ppm

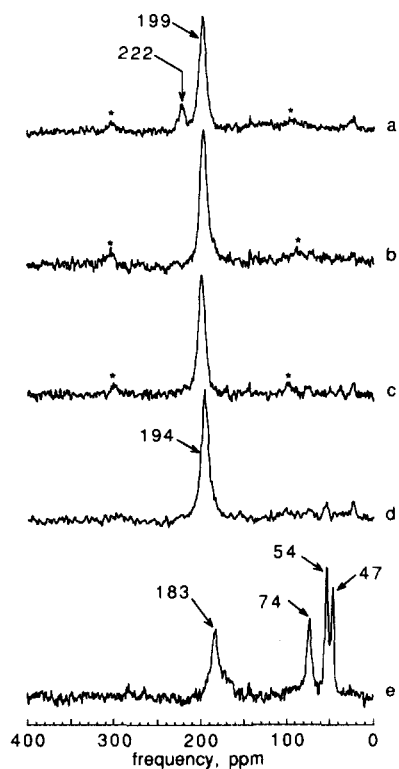
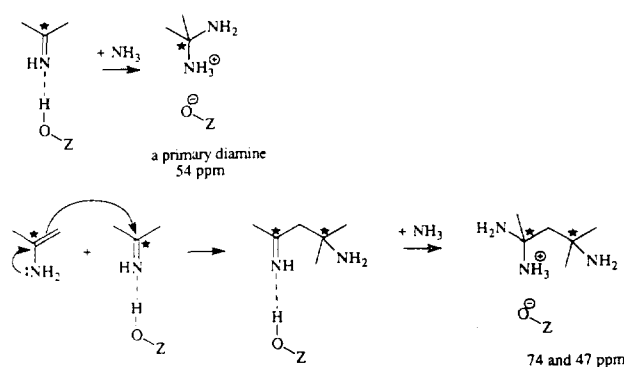


FIG. 3. CPMAS spectra (4096 scans) of 0.5 acetone molecule per Brønsted site adsorbed on H-ZSM-5(B), followed by exposure to (a) 0.5  $\text{NH}_3$  molecules per site, MAS frequency 3.0 kHz; (b) 1.0  $\text{NH}_3$  molecules per site, MAS frequency 3.0 kHz; (c) 1.5  $\text{NH}_3$  molecules per site, MAS frequency 2.9 kHz; (d) 2.6  $\text{NH}_3$  molecules per site, MAS frequency 3.0 kHz; and (e), saturated with  $\text{NH}_3$ , MAS frequency 3.0 kHz.



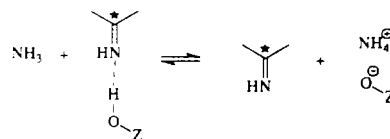
SCHEME 5. Formation of primary amines from 2-propanimine and ammonia.

to chloroacetone is supported by the spectrum in Fig. 2c of 0.70 molecule of chloroacetone adsorbed on H-ZSM-5.

#### Formation of Imines from Acetone and Ammonia

The properties of the chemisorbed acetone molecule at room temperature allow the formation of 2-propanimine on exposure to ammonia (5, 9) (Scheme 4). Figure 3a is the CPMAS spectrum following exposure of the H-ZSM-5(B) sample at 295 K to 0.5 molecule of acetone per Brønsted site, followed by exposure to 0.50 molecule of ammonia per site. The spectrum shows unreacted acetone (222 ppm) and a feature at 199 ppm which we assign to 2-propanimine chemisorbed at the acid site. Since the proton affinity of the imine is considerably larger than that of aldehydes and ketones (24), the adsorption complex at the Brønsted site in this case is in all probability protonated, as in the magic-acid solutions of Olah (25). The reaction goes to completion following addition of an excess of ammonia. The spectra for 1.0 and 1.5 molecules of ammonia per site are shown in Figs. 3b and 3c.

As shown in Scheme 5, addition of extra ammonia should lead to the formation of diamines. This can be seen in Figs. 3d and 3e, which show the results of investigations on the reaction of imines with ammonia. At a coverage of 2.6 molecules of ammonia per Brønsted site (Fig. 3d), we observe a feature at 54 ppm which we assign to a diamine. The feature at 194 ppm probably corresponds to the initial imine which is now competing with the large excess of ammonia for the Brønsted sites. When equilibrium is established (Scheme 6), measurable con-



SCHEME 6. Equilibrium exchange of ammonia and 2-propanimine.

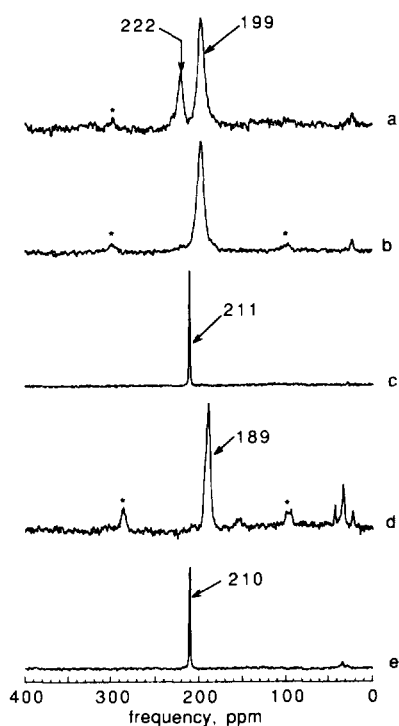


FIG. 4. MAS spectra (4096 scans) at 3.7 kHz for 0.5 acetone molecules per Brønsted site, added to H-ZSM-5(B) containing (a) 0.5  $\text{NH}_3$  molecules per site, CP; (b) 1.0  $\text{NH}_3$  molecules per site, CP. Spectrum (d) was obtained with CP after sequential exposure of H-ZSM-5 to 0.5 molecule of acetone per site and 1.0 molecule of dimethylamine per Brønsted site. Spectra (c) and (e) were taken on the same samples as in (b) and (d), respectively, with a Hahn echo after exposure to ambient air overnight using 16,384 points in the acquisition.

centrations of both the imine and the iminium ion are present and the chemical shift represents an average given by the equilibrium concentrations in the zeolite. In Fig. 3e, where we have saturated the sample with ammonia, we see the formation of two additional features corresponding to primary amines at 74 and 47 ppm (Scheme 5), as well as a further upfield shift in the imine feature to 183 ppm.

Reversing the procedure by first adding the ammonia to the zeolite and then acetone to form ammonium ions does not change the products but only the extent to which the reaction goes to completion. Figure 4a shows the results after dosing the zeolite with 0.50 molecule of ammonia per Brønsted site, followed by dosing with 0.50 molecule of acetone per acid site. The only change from the spectrum in Fig. 3a is in the amount of unreacted acetone present. The reaction again goes to completion at higher ammonia loading, as seen in Fig. 4b. The difference in the behavior of H-ZSM-5 and  $\text{NH}_4$ -ZSM-5 (Scheme 7) in the formation of the imine appears to be the rate of reaction.

For each of the above preparations, the exposure of

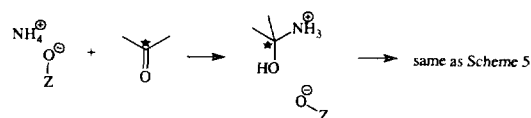
the chemisorbed imines to water results in rapid dehydration of the imine to regenerate acetone, as in aqueous solutions (26). This is shown in Fig. 4c, where the feature at 211 ppm corresponds to acetone adsorbed on H-ZSM-5 saturated with water. The character of the acetone complex in the H-ZSM-5 is considerably altered with respect both to the downfield shift relative to the pure liquid and to its mobility in the zeolite. In fact, it more closely resembles the liquid than a hydrogen-bonded precursor to a carbocation.

The spectrum in Fig. 4d shows that exposure of chemisorbed acetone to dimethylamine results in the formation of *N,N*-dimethyl-2-propaniminium ions. The chemical shift of this species is again consistent with what has been observed by Olah in magic-acid solutions (25). As with the 2-propaniminium ions examined above, this species is unstable in the presence of water and rapidly rehydrates to acetone (Fig. 4e).

#### Reactions of Acetaldehyde

Figure 5a is the spectrum following exposure at 295 K of the H-ZSM-5(B) sample to 0.5 molecule of  $^{13}\text{C}$  isotopically enriched acetaldehyde per Brønsted acid site. The spectrum shows primarily the downfield-shifted two carbon atoms of unreacted acetaldehyde forming an adsorption complex at 212 and 29 ppm, with weak features at 203, 178, 134, and 19 ppm which probably correspond to crotonaldehyde. This is the expected product of the aldol condensation reaction of acetaldehyde, as shown in Scheme 8. Like the acetone case, downfield shifts for acetaldehyde suggest a hydrogen-bonded precursor to a carbocation at low surface coverage. Unlike acetone, however, the adol products cannot be entirely suppressed, even for low surface coverage sample preparations at 0°C. Again assuming that mobility of the adsorption complex is the primary factor leading to bimolecular products, the localization of the acetaldehyde complex must be incomplete. This is supported by the broadline spectrum in the absence of MAS, shown in Fig. 6, where a comparison with acetone, at the same surface coverage and temperature, shows a considerably reduced anisotropy from the nearly rigid lattice form of acetone.

The effects of temperature and surface coverage are shown in Figs. 5b through 5d. The sample in Fig. 5b is the same as that in Fig. 5a, except that the sample was heated to 100°C for 30 min. Figure 5c was obtained at an



SCHEME 7. Reaction of acetone with  $[\text{NH}_4]$ -ZSM-5.

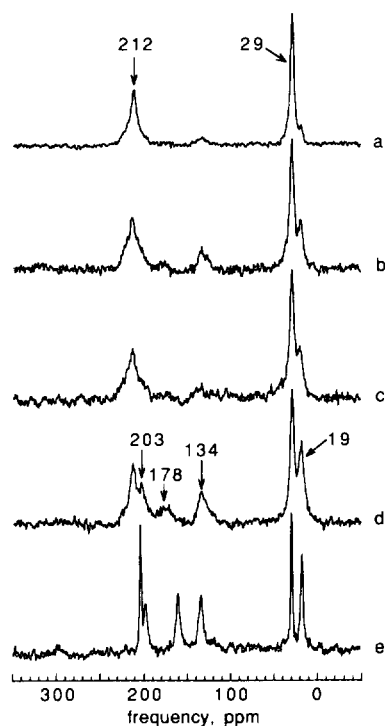
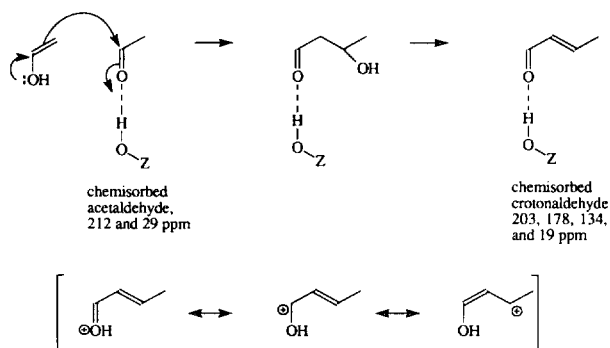


FIG. 5. CPMAS spectra at 3.2 kHz of acetaldehyde on H-ZSM-5(B). (a) 0.5 molecule per site, 8192 scans; (b) 0.5 molecule per site, heated to 100°C for 30 min; (c) 0.88 molecule per site; (d) 0.88 molecule per site, heated to 100°C for 30 min; and (e) same sample as in (d) following exposure to ambient air overnight.

acetaldehyde concentration of 0.88 molecule per Brønsted site without heating. Figure 5d shows the spectrum of a sample with a surface coverage of 0.88 molecule per acid site, prepared at room temperature and heated to 100°C for 30 min. It is apparent that increasing either the temperature or the surface coverage, both of which should increase the mobility of the adsorption complex, leads to an increase in the concentration of the initial condensation product, crotonaldehyde. Comparison of the spectra in



SCHEME 8. Formation of crotonaldehyde from acetaldehyde.

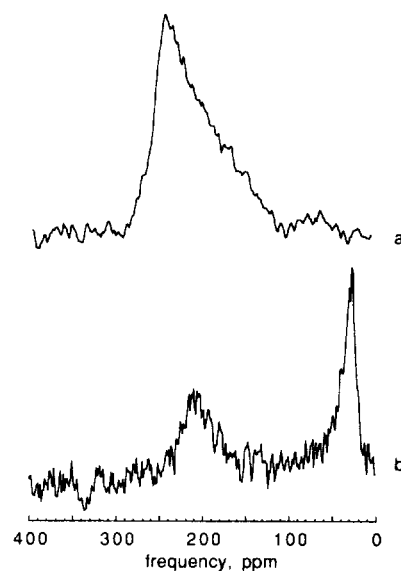


FIG. 6. Hahn echo spectra in the absence of MAS, for (a) acetone (28,320 scans, same as Fig. 2b in Ref. (7)), and (b) acetaldehyde (7980 scans) at 0.85 molecule per site on H-ZSM-5(A).

Fig. 5 with those of Haw *et al.* (27) suggests that high acetaldehyde loadings caused bimolecular reactions to dominate the spectra in that study (see Fig. 1 in Ref. (27)).

The reactions of acetaldehyde and crotonaldehyde with ammonia to form imines were also investigated. The sample H-ZSM-5(B) was first exposed to 0.5 molecule of acetaldehyde per Brønsted acid site and then to an amount of ammonia corresponding to 0.5 molecule per acid site. The spectrum immediately after exposure to ammonia is shown in Fig. 7a. We observe features at 186 ppm which we assign to the C-1 carbon of ethanimine, as well as features at 175, 164, 125, and 27 ppm, assigned to 2-butenimine. The large feature centered at 27 ppm is probably due to the convolution of features due to the CH<sub>3</sub> groups in ethanimine and 2-butenimine. The 2-butenimine could be formed by either the reaction of ammonia with the carbonyl carbon of crotonaldehyde or the condensation of ethanimine with its enamine form. All of these reactions are outlined in Scheme 9. The feature at 67 ppm decays with time, as seen in Figs. 7b and 7c, and may be due to the presence of a carbinolamine, the dehydration of which is usually considered to be the rate-limiting step in reactions of this type (26), although not observed in the reactions of acetone with ammonia. Further evidence for the condensation reactions of ethanimine and its enamine tautomer is the increase with time of the features at 29 and 48 ppm, which are due to primary amines, which can form only in the presence of excess ammonia. Since we started with stoichiometric amounts of acetaldehyde and ammonia, this excess ammonia must be coming from the formation of condensation products.



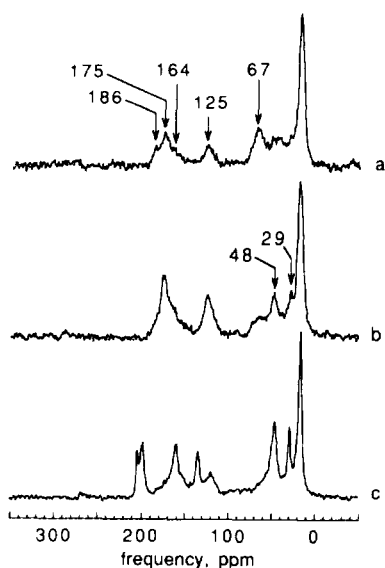


FIG. 7. CPMAS spectra (4096 scans) at 3.7 kHz following sequential exposure of H-ZSM-5(B) to 0.5 molecule of acetaldehyde and then (a) 0.5 molecule of ammonia. Spectrum (b), same sample as in (a), taken 3 h later. Spectrum (c), same as in (b) after exposure to ambient air overnight.

As in the case of imines formed from acetone, the imines formed from acetaldehyde and crotonaldehyde are not stable in the presence of large amounts of water. The spectrum following equilibration of the sample in ambient air is shown in Fig. 7c. As can be seen in Fig. 7c, features appear at 205, 200, 160, 133, 25, and 19 ppm, corresponding to a mixture of acetaldehyde and crotonaldehyde, as discussed above.

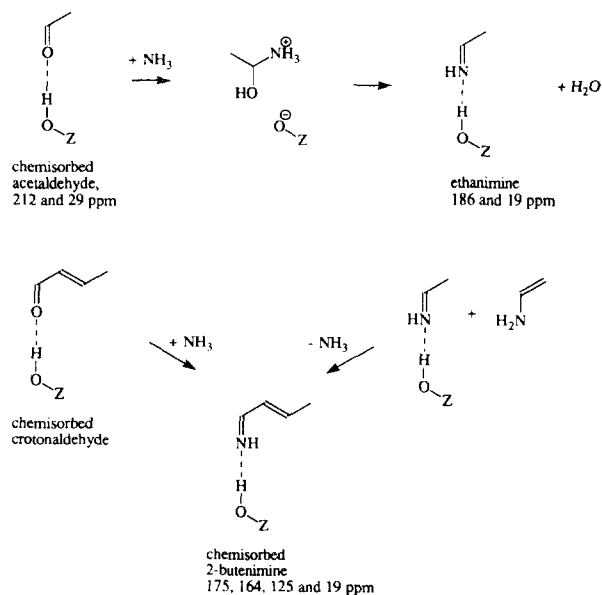
## DISCUSSION

### Factors Affecting the Rate of Primary Condensation Reactions

The present results together with our earlier studies (6, 7) and those of Bosacek *et al.* (8, 9) and of Haw *et al.* (10) provide some clarification of the important factors that lead to the onset and rate of condensation reactions in a high-activity, unpoisoned zeolite such as H-ZSM-5. The initial step in the condensation reaction of chemisorbed carbonyl compounds is clearly the formation of a hydrogen-bonded precursor to a carbocation, which is quite stable when conditions during, and following, sample preparation are such as to localize the complex in a time scale that is long compared to that for site exchange. In the case of acetone, it can be seen from our studies, as well as those of Bosacek *et al.* (8, 9), that localization in the absence of significant site exchange is easily achieved at room temperatures,  $\sim 300$  K, at surface cover-

ages corresponding to less than one molecule per Brønsted site. What is noteworthy is that the shift anisotropy of these surface complexes appears to be identical in the three different H-ZSM-5 samples used in our studies, not only from the standpoint of the isotropic shifts (17 ppm + 0.4 ppm downfield from pure solid acetone), but also from the apparent elements of the chemical shift tensor in the rigid lattice (6, 7) which are far more sensitive to changes in the charge density of the adsorbed molecule due to the surface environment. This lack of sensitivity of the chemical shift at low surface coverages to sample preparation is also apparent in the H-ZSM-5 samples of Bosacek *et al.* (8, 9), as well as those of Xu *et al.* (10).

To initiate the condensation reactions (a bimolecular process) at low surface coverage, delocalization of some fraction of the complexes by site exchange is necessary. Using  $^{13}\text{C}$  NMR, the time scale for site exchange, and thus conditions when site exchange becomes sufficiently rapid to permit observable products of condensation reactions, cannot be determined without a detailed knowledge of the mechanisms contributing to the reorientational correlation times associated with changes in lineshape of the chemical shift anisotropy as a function of both temperature and surface coverage. Although we have yet to complete such studies for the acetone complex, it is clear from our earlier lineshape studies (6, 7) and the condensation reactions reported here that molecular reorientations by site exchange do become significant, even at room temperature, for surface coverages above one molecule per Brønsted site. But it is also evident from the present studies, as well as those of Bosacek *et al.* (8, 9), that



SCHEME 9. Formation of imines from acetaldehyde, crotonaldehyde, and ammonia.

thermally activated site exchange leading to condensation products of acetone can also occur at low surface coverages, below one molecule per Brønsted site; however, the lower the surface coverage, the higher the temperature required for a given rate of formation of condensation products.

A comparison of the lineshape of the acetone complex with that of acetaldehyde at a surface coverage of 0.8 molecule per site and 295 K (see Fig. 6) would suggest that motional narrowing due to reorientations is considerably greater in the latter than in the former. Neither, however, exhibit appreciable condensation products in the time scale of  $\sim 1$  h, indicating that the anisotropic motional narrowing is not always a criterion for site exchange. Neither is the rigid lattice lineshape the only criterion for Brønsted site localization since, from Fig. 6, anisotropic reorientations can also occur when the complex (acetaldehyde) is still highly localized (a rotational diffusion). Dynamically, what differentiates the acetone complex from the acetaldehyde complex is the lower strength of the hydrogen bonding as well as steric factors, such as the size of the adsorbed molecule relative to the zeolite channel size, which determines the barriers to rotation (7).

A useful quantitative scale in the comparison of zeolites is what Xu *et al.* (10) have referred to as the "reactivity" with respect to a given condensation reaction; presumably, the rate of reaction under some specified *standard* set of conditions. From the discussion above, it is clear that such conditions, which depend on both temperature and surface coverage in the case of the primary condensation reactions, must somehow relate to the rate of site exchange, an important factor in the rate. Using  $^{13}\text{C}$  NMR techniques, we are now exploring the conditions which will permit a quantitative assessment of reactivity. We believe these can be obtained from the rigid lattice shift anisotropy of a probe molecule (which measures the extent of proton transfer, that is, the zeolite "acidity") and the temperature dependence of the anisotropic lineshapes of the "complexed" reactants and products (which relate to orientational barriers).

#### *Elementary Processes in Condensation Reactions of Acetone and Acetaldehyde on H-ZSM-5*

The reactions described in Schemes 1 through 9 of this paper, some of which have been recently proposed by Xu *et al.* (10), are very similar to those observed in solution-phase acids. The products and intermediates appear to be closely related. The reaction of  $\text{Cl}_2$  with the enol form of acetone, the condensation reactions to form mesityl oxide and crotonaldehyde, and the nucleophilic attack of the carbonyls by ammonia and amines all occur in solution phase. In both zeolite and solution-phase media, the condensations are initiated by a deshielding of the

carbonyl carbon which leads to a substantial positive charge on that atom.

From a microscopic point of view, however, one can expect significant differences in the reaction coordinates describing the reaction pathways in zeolites from those in liquid solutions. This is mainly due to the absence of solvation effects in the case of zeolites. Dynamically the frequency and amplitude of the random thermal fluctuations necessary for classical barrier crossing cannot be the same in the two cases; nor can the barrier heights or activation energies be the same. Unfortunately the NMR time scales are too long to observe such events. However, it is clear from the behavior of the equilibrated hydrogen-bonded complex at the Brønsted sites that the fluctuations of the delocalized proton, mediated by framework phonons, are not so large as to lead to exchange between a protonated and unprotonated form of the complex, events observable in liquid solutions.

An interesting feature of the present results is the estimation of the enol lifetime in the chlorination reaction, as shown in Scheme 3, based on the assumption that the rate-limiting step is the formation of the enol complex. Its order of magnitude is similar to that of the keto-enol reaction rate in solutions where the Hammett acidity is in the range of  $-3$  to  $-4$  (23), similar to what one would expect for trifluoroacetic acid.

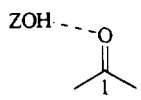
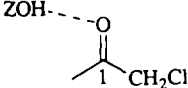
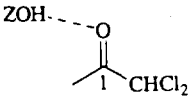
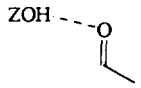
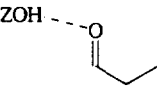
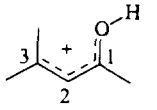
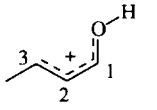
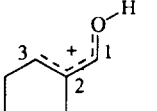
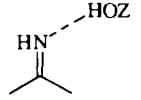
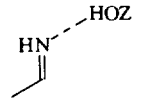
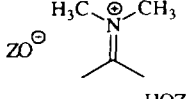
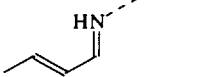
One reaction which did show differences in the behavior of the zeolite relative to solutions was the formation of 2-propanimine from acetone and ammonia. In solution-phase acids, the rate at low pH (low ammonia concentration) is limited by the concentration of free nucleophile, ammonia (26). However, in the ammonium form where no free nucleophile exists, the reaction of acetone occurs readily. Since the heat of adsorption of ammonia at the Brønsted sites is 145 kJ/mol (30), compared to only  $\sim 120$  kJ/mol for acetone (31), this can be accounted for by a unimolecular rearrangement of an acetone-ammonium complex at the Brønsted sites rather than a displacement of the ammonium ion to form a free nucleophile.

#### *Adsorption Complexes of Acetone, Acetaldehyde, and Their Primary Condensation Products*

The adsorption complexes corresponding to a number of important organic molecules were examined in the course of this study, as listed in Table 1. The complexes are stable structures formed by hydrogen bonds between the Brønsted site and the adsorbate. The isotropic chemical shifts indicate the extent to which the nucleus has been deshielded by the formation of the hydrogen bond.

For the molecules with high proton affinities like the imines (for example, *N*-ethylethanamine has a proton affinity of 222.8 kcal/mol, compared to 225.1 kcal/mol for diethylamine (24)), the isotropic chemical shifts are almost

TABLE 1  
Chemical shifts of Protonated or Partially Protonated Intermediates

Species	$\delta(C-1)$	$\delta(C-3)$
	222 <sup>a,b</sup> 224 <sup>c</sup> 224 <sup>d</sup> 205 <sup>e</sup> 249 <sup>f</sup>	
	206 <sup>a</sup> 200 <sup>e</sup>	
	197 <sup>a</sup> 195 <sup>e</sup>	
	212 <sup>a</sup> 201 <sup>d</sup> 200 <sup>e</sup> 235.1 <sup>f</sup>	
	214 <sup>g</sup> 200 <sup>e</sup>	
	210 <sup>a</sup> 210 <sup>c</sup> 210 <sup>d</sup> 195.9 <sup>e</sup> 215.5 <sup>f</sup>	188 <sup>a</sup> 187 <sup>c</sup> 187 <sup>d</sup> 152.5 <sup>e</sup> 181.8 <sup>f</sup>
	203 <sup>a</sup> 198 <sup>d</sup> 191.1 <sup>e</sup> 206 <sup>f</sup>	178 <sup>a</sup> 162 <sup>d</sup> 151.8 <sup>e</sup> 201 <sup>f</sup>
	205 <sup>g</sup>	180 <sup>g</sup>
	199 <sup>a</sup> 200 <sup>c</sup> 201.6 <sup>f</sup>	
	186 <sup>a</sup> 189.5 <sup>f</sup>	
	189 <sup>a</sup> 189.5 <sup>f</sup>	
	175 <sup>a</sup>	160 <sup>a</sup>

<sup>a</sup> This study.

<sup>b</sup> The trace of the chemical shielding tensor was originally reported by us as 224 ppm (6); this has since been corrected (7).

<sup>c</sup> From Kubelkova *et al.* (6, 7).

<sup>d</sup> From Haw *et al.* (10, 27). Acetone, Ref. (10). Acetaldehyde, Ref. (27).

<sup>e</sup> Pure liquid.

identical to those observed for similar, hydrogen-bonded complexes in magic-acid solutions (25). In these cases, the proton is almost completely transferred to the molecule in both the complex at the acid site in the zeolite and the magic-acid solution. For molecules with lower proton affinities, such as acetone and acetaldehyde (proton affinities of 197.2 and 188.9 kcal/mol, respectively), the isotropic chemical shifts in the zeolite are significantly different from that observed in magic acids. For these, the downfield <sup>13</sup>C chemical shifts relate to the extent of proton transfer in the complex.

A closer examination of the results in Table 1 indicates some interesting features for mesityl oxide and crotonaldehyde. These molecules should have a larger proton affinity than acetone or acetaldehyde due to resonance stabilization of the protonated species, as shown in Schemes 2 and 8, and, therefore, their isotropic shifts in the zeolite are closer to the results observed in magic acids (i.e., the extent of protonation in these molecules is more complete). The resonance stabilization of the carbocation also leads to a positive charge and a large downfield shift in the beta carbon (C-3) resonance as well as that of the carbonyl carbon (C-1). However, it is noteworthy that the magnitude of the chemical shifts for the C-1 and C-3 carbons for these molecules is not identical to that reported in solutions, suggesting that the distribution of charge on the molecules is different in the zeolite. For crotonaldehyde, the chemical shift for the C-1 carbon is practically identical to that observed in magic acids (14 ppm versus 15 ppm), but the isotropic shift for the C-3 carbon, still large at 26 ppm, is significantly less than that observed in magic acids, 49 ppm. The difference with mesityl oxide is more apparent. The isotropic shift for the C-1 carbon in the zeolite (14 ppm) is less than that observed in magic acid (20 ppm), while the chemical shift for C-3 in the zeolite is larger, 35 ppm downfield from the pure compound compared to only 29 ppm in magic acid. Since strong solvation effects could strongly influence the carbocations in solution (32) and multiple hydrogen bonds could form in the zeolite, it is not surprising that these differences exist.

The <sup>13</sup>C chemical shift of mesityl oxide adsorbed in zeolites has been suggested for use as a probe of acidity, assuming that the chemical shift reflects the concentration of protonated and unprotonated species (10, 33). While there is no equilibrium between such species in the H-ZSM-5 at low coverages, the <sup>13</sup>C chemical shifts are nevertheless a reasonable measure of the extent of proton

<sup>f</sup> From Olah, *et al.* Acetone, acetaldehyde, Ref. (28). Imines, Ref. (25). Unsaturated aldehydes and ketones, Ref. (20).

<sup>g</sup> From Biaglow *et al.* (34). The formation of propanal and its subsequent condensation products at the acid sites were postulated in Ref. (34). The chemical shift of the carbonyl carbon of propanal was estimated from overlapping features at ~216 ppm in Ref. (34).

transfer and, thus, like acetone (6, 7), provide a method for distinguishing between different acid sites in zeolites.

### CONCLUSIONS

(1) Using  $^{13}\text{C}$  NMR, the primary processes for the bimolecular, acid-catalyzed condensation reactions involving acetone and acetaldehyde in H-ZSM-5 can be observed. The rates of reaction are, however, critically dependent on the surface coverage and temperature (8–10, 27).

(2) With few exceptions, the initial products of the condensation chemistry in H-ZSM-5 are the same as the those in liquid solutions.

(3) The formation of protonated imines by exposure of the adsorption complexes to amines occurs readily at room temperature. This reaction appears to differ from that observed in solution phase in that the reaction is not inhibited by formation of ammonium ions.

(4) The presence of an enol form of acetone adsorbed in H-ZSM-5 was confirmed in the reaction with  $\text{Cl}_2$ .

(5) The  $^{13}\text{C}$  chemical shifts of the reactant and condensation product adsorption complexes observed in this study can be described in terms of hydrogen bonding at the acid sites. The extent of proton transfer in each of the complexes can be related to the  $^{13}\text{C}$  downfield chemical shifts relative to the pure liquids.

### ACKNOWLEDGMENTS

This work was supported by NSF Grant CTS91-01447. The authors also acknowledge the many helpful discussions of this work with W. Daley, G. Voth, and M. Klein. We also thank Maura Mimnaugh for help with the chlorination experiments.

### REFERENCES

- Scheidt, F. M., *J. Catal.* **3**, 372 (1964).
- Reichle, W. T., *J. Catal.* **63**, 295 (1980).
- Chang, C. D., and Silvestri, A. J., *J. Catal.* **47**, 249 (1977).
- Baigrie, L. M., Cox, R. A., Slebocka-Tilk, H., Tencer, M., and Tidwell, T. T., *J. Am. Chem. Soc.* **107**, 3640 (1985).
- Carey, F. A., and Sundberg, R. J. "Advanced Organic Chemistry," p. 447. Plenum, New York, 1990.
- Biaglow, A. I., Gorte, R. J., and White, D., *J. Phys. Chem.* **97**, 7135 (1993).
- Biaglow, A. I., Gorte, R. J., Kokotailo, G. T., and White, D., *J. Catal.* **148**, 779 (1994).
- Bosacek, V., and Kubelkova, L., *Zeolites* **10**, 64 (1990).
- Bosacek, V., Kubelkova, L., and Novakova, J., *Stud. Surf. Sci.* **65**, 337 (1991).
- Xu, T., Munson, E. J., and Haw, J. F., *J. Am. Chem. Soc.* **116**, 1962 (1994).
- Kofke, T. J. G., Gorte, R. J., and Farneth, W. E., *J. Catal.* **114**, 34 (1988).
- Aronson, M. T., Gorte, R. J., and Farneth, W. E., *J. Catal.* **98**, 434 (1986).
- Parrillo, D. J., Adamo, A. T., Kokotailo, G. T., and Gorte, R. J., *Appl. Catal.* **67**, 107 (1990).
- Kofke, T. J. G., Gorte, R. J., Kokotailo, G. T., and Farneth, W. E., *J. Catal.* **115**, 265 (1989).
- Maciel, G. E., and Natterstad, J. J., *J. Chem. Phys.* **42**, 2752 (1965).
- White, D., Evleth, E., Kassab, V., and Allevina, M., unpublished calculations.
- Pulay, P., Dept. of Chemistry and Biochemistry, University of Arkansas, Fayetteville, Arkansas, 72701.
- Rollman, L. S., and Valyocsik, E. W., *Inorg. Synth.* **61**, 22 (1983).
- Biaglow, A. I., Gorte, R. J., and White, D., *J. Catal.*, **150**, 221 (1994).
- Olah, G. A., Halpern, Y., Mo, Y. K., and Liang, G., *J. Am. Chem. Soc.* **94**, 3554 (1972).
- Suwelack, D., Rothwell, W. P., and Waugh, J. S., *J. Chem. Phys.* **73**, 2559 (1980).
- Schaefer, J., Stejskal, E. O., and Buchdahl, R., *Macromolecules* **10**, 384 (1977).
- McTigue, P. T., and Sime, J. M., *Aust. J. Chem.* **20**, 905 (1967).
- Aue, D. H., and Bowers, M. T., in "Gas-Phase Ion Chemistry" (M. T. Bowers, Ed.), pp. 2–47. Academic Press, New York, 1979.
- Olah, G. A., and Donovan, D. J., *J. Org. Chem.* **43**, 860 (1978).
- Streitwieser, A., and Heathcock, C. H., "Introduction to Organic Chemistry," p. 383. MacMillan, New York, 1983.
- Munson, E. J., and Haw, J. F., *Angew. Chem., Int. Ed. Engl.* **32**, 615 (1993).
- Olah, G. A., and White, A. M., *J. Am. Chem. Soc.*, **91**, 5801 (1969).
- Guillemin, J. C., and Denis, J. M., *Tetrahedron* **44**, 4431 (1988).
- Parrillo, D. J., Lee, C., and Gorte, R. J., *Appl. Catal. A* **110**, 67 (1994).
- Lee, C., and Gorte, R. J., unpublished data.
- Parrillo, D. J., Gorte, R. J., and Farneth, W. E., *J. Am. Chem. Soc.* **115**, 12441 (1993).
- Farcasiu, D., Ghenciu, A., and Miller, G., *J. Catal.* **134**, 118 (1992).
- Biaglow, A. I., Gorte, R. J., and White, D., *JCS Chem. Comm.*, **1164** (1993).